





Alterations of retinal thickness measured by optical coherence tomography correlate with neurophysiological measures in diabetic polyneuropathy

Yuichiro Yamada¹, Tatsuhiro Himeno¹ , Kotaro Tsuboi², Yuka Shibata^{1,3}, Miyuka Kawai¹ , Yuriko Asada-Yamada¹, Yusuke Hayashi¹, Emi Asano-Hayami¹, Tomohide Hayami¹ , Yuichiro Ishida², Yohei Ejima¹, Mikio Motegi¹, Saeko Asano¹, Makoto Kato¹, Eriko Nagao¹, Hiromi Nakai-Shimoda¹, Takahiro Ishikawa¹, Yoshiaki Morishita¹, Masaki Kondo¹ , Shin Tsunekawa¹, Yoshiro Kato¹, Takayuki Nakayama⁴, Motohiro Kamei², Jiro Nakamura¹, Hideki Kamiya^{1*}

¹Division of Diabetes, Department of Internal Medicine, Aichi Medical University School of Medicine, Nagakute, Japan, ²Department of Ophthalmology, Aichi Medical University School of Medicine, Nagakute, Japan, ³Department of Laboratory, Aichi Medical University Clinic, Nagoya, Japan, ⁴Department of Clinical Laboratory, Aichi Medical University Hospital, Nagakute, Japan

Keywords

Diabetic polyneuropathies,
Neuroretina

*Correspondence

Hideki Kamiya
Tel.: +81-561-63-1683
Fax: +81-561-63-1276
E-mail address:
hkamiya@aichi-med-u.ac.jp

J Diabetes Investig 2021; 12:
1430–1441

doi: 10.1111/jdi.13476

ABSTRACT

Aims/Introduction: Diabetic polyneuropathy (DPN) and diabetic retinopathy (DR) are traditionally regarded as microvascular complications. However, these complications may share similar neurodegenerative pathologies. Here we evaluate the correlations in the severity of DPN and changes in the thickness of neuroretinal layers to elucidate whether these complications exist at similar stages of progression.

Materials and Methods: A total of 43 patients with type 2 diabetes underwent a nerve conduction study (NCS), a macular optical coherence tomography, and a carotid artery ultrasound scan. Diabetic polyneuropathy was classified according to Baba's classification using NCS. The retina was automatically segmented into four layers; ganglion cell complex (GCC), inner nuclear layer/outer plexiform layer (INL/OPL), outer nuclear layer/photoreceptor inner and outer segments, and retinal pigment epithelium (RPE). The thickness of each retinal layer was separately analyzed for the fovea and the parafovea.

Results: Fourteen patients were classified as having moderate to severe diabetic polyneuropathy. The thicknesses of the foveal and parafoveal INL/OPL increased in patients with diabetic polyneuropathy compared with patients without. The thickness of the parafoveal retinal pigment epithelium decreased in patients with diabetic polyneuropathy. The thinning of parafoveal ganglion cell complex and foveal and parafoveal retinal pigment epithelium were positively correlated with deterioration of nerve functions in the nerve conduction study, but the thickening of INL/OPL was positively correlated with the nerve function deterioration. The thinning of parafoveal ganglion cell complex and foveal retinal pigment epithelium were positively correlated with the thickening of the carotid intima-media.

Conclusions: Depending on the progression of diabetic polyneuropathy, the ganglion cell complex and retinal pigment epithelium became thinner and the INL/OPL became thicker. These retinal changes might be noteworthy for pathological investigations and for the assessment of diabetic polyneuropathy and diabetic retinopathy.

Received 22 September 2020; revised 1 December 2020; accepted 4 December 2020

INTRODUCTION

Among the many chronic diabetic complications and comorbidities, diabetic retinopathy (DR), diabetic polyneuropathy (DPN), and diabetic kidney disease (DKD) are traditionally regarded as the three major 'microvascular' complications¹. Diabetic retinopathy, in particular – according to the conventional hypothesis – is mainly caused by pathological angiogenesis, by which newly developed vessels are immature, fragile, and easily hemorrhagic. However, considering the fact that the site primarily affected by diabetic retinopathy is the neuroretina, an alternative hypothesis has been developed. As the neuroretina has an intimate relationship with the vascular system, the concept of a neurovascular unit, which was originally proposed in the brain, has also been applied to the retina². In this context, a novel hypothesis has been proposed that the dysfunction of the neurovascular unit prior to vasculopathy is one of the pathological aspects of diabetic retinopathy^{3,4}. To support this hypothesis, many researchers have reported that neural cell death and thinning in the ganglion cell complex (GCC) occurred from an early stage of diabetes, which existed before the vascular changes^{5–12}. Furthermore, in a rodent model of diabetes, metabolic abnormalities in retinal neurons and glial cells have been indicated¹³.

Optical coherence tomography (OCT), which is a non-invasive ophthalmic imaging technique, allows us to obtain three-dimensional retinal volume data and high-resolution cross-sectional images. As optical coherence tomography is non-invasive and quick to perform, ophthalmologists generally use it for the assessment and treatment of retinal diseases. Furthermore, a correlation between the findings in optical coherence tomography and the pathology of neurodegenerative diseases has been pointed out; retinal neurodegeneration in Alzheimer's disease^{14,15}, Parkinson's disease¹⁶, and mild cognitive impairment¹⁷ have been reported. However, although various findings have been accumulated to elucidate the pathology of diabetic retinopathy based on the neurovascular unit hypothesis^{18–20}, the point of view that neurodegeneration in diabetic retinopathy might be an aspect of another important diabetic complication of diabetic polyneuropathy has not been investigated fully. Most previous reports about the relationship between diabetic polyneuropathy and retinal neurodegeneration used non-quantitative physical findings of diabetic polyneuropathy, e.g., the Neuropathy Disability Score (NDS), but not quantitative assessments of diabetic polyneuropathy including a nerve conduction study (NCS)^{21–23}. In previous reports, thinning of the retinal nerve fiber layer (RNFL) around the optic disc and partial thinning in ganglion cell complex around the fovea were observed with the progression of diabetic polyneuropathy^{22,23}. Additionally, Hafner *et al.*²⁴ recently reported that the reduction of peripapillary retinal nerve fiber layer thicknesses was correlated with quantitative findings of small fiber neuropathy, i.e., intraepidermal nerve fiber density and findings in the corneal nerve fiber. As the retinal nerve fiber layer is composed of

axons of retinal ganglion cells in the ganglion cell complex, or third-order neurons in the neuroretina, it was indicated that retinal neurodegeneration caused by diabetes might mainly impair retinal ganglion cells.

However, retinal cells other than ganglion cells, including the photoreceptor cells (the first-order neurons or paraneurons) and the second-order neurons in the inner nuclear layer (INL) have not been studied in depth as a component of neurodegeneration in diabetic polyneuropathy. Therefore, the magnitude of neuroretinal impairment as a pathological aspect in diabetic polyneuropathy is not yet clear. In this study, we aimed to evaluate the correlation between the degree of neurodegeneration in the retina and the nerve conduction test, a quantitative test of diabetic polyneuropathy. The changes in the thickness of each retinal layer around the macula, which is expected to be the best location to evaluate the neuroretina²⁵, were elucidated in detail using optical coherence tomography.

MATERIALS AND METHODS

Subjects

From 2018 to 2019, all patients who had been previously diagnosed as having type 2 diabetes mellitus and who were hospitalized at Aichi Medical University Hospital to improve their hyperglycemia were invited to the study. Forty-three subjects who signed a document of consent for the study were enrolled. Exclusion criteria were patients having the following conditions: macula edema, glaucoma, cataract that prevented satisfactory retinal imaging, a history of retinal photocoagulation, a history of intraocular pressure above 22 mmHg, Parkinson's disease, multiple sclerosis, diabetic ketoacidosis, severe infection, or severe injuries. The characteristics of the patients were assessed by physical findings, sociodemographic information, and laboratory measurements including serum creatinine, serum urea nitrogen, urinary albumin-to-creatinine ratio (u-ACR), urinary liver-type fatty acid-binding protein, fasting blood glucose, glycoalbumin, glycosylated hemoglobin (HbA1c), high-density lipoprotein (HDL), low-density lipoprotein (LDL), and triglyceride (TG). Diabetic nephropathy was categorized as stage 1–5 based on the classification of diabetic nephropathy established in 2014 by the Joint Committee on Diabetic Nephropathy, in which the estimated glomerular filtration rate (eGFR) and u-ACR were employed for the staging²⁶. The eGFR was calculated using the equations for eGFR developed by the Japanese Society of Nephrology²⁷. The carotid intima-media thickness (IMT), plaque prevalence at the carotid artery, ankle-brachial index (ABI), toe-brachial index (TBI), and brachial-ankle pulse wave velocity (baPWV) were evaluated. The data of participants without diabetes were collected retrospectively using an opt-out approach. The characteristics of the patients without diabetes were assessed by physical findings, sociodemographic information, and laboratory measurements including serum creatinine, serum urea nitrogen, casual blood glucose, total cholesterol, and triglyceride. Study procedures were approved by the ethics com-

mittee of Aichi Medical University Hospital (2017-H007). The study was conducted in accordance with the Declaration of Helsinki.

OCT

Optical coherence tomography images were obtained using a commercial 70 kHz spectral domain OCT (RTVue XR Avanti, Optovue Inc, Fremont, CA, USA) with a center wavelength of 840 nm and Angio Vue software (version 2017.1.0.155; Optovue Inc). The 3×3 mm macular cube scan images centered on the fovea were captured by certified photographers who were unaware of the clinical backgrounds of each patient. The macula lutea is anatomically and functionally divided into three regions: the fovea, the parafovea, and the perifovea. As the fovea contains the foveal avascular zone, whereas the parafovea has the thickest neuroretina in the retina, the fovea and the parafovea were analyzed separately. The thickness of each retinal layer was measured along four radial lines and two circles centered at the fovea based on the Early Treatment Diabetic Retinopathy Study (ETDRS) grid²⁸. The inner zone, which was the same as the center fovea subfield of the ETDRS grid, including the fovea, was defined as within a 1 mm circle. The outer region, or the parafoveal zone, was defined by the area between an inner circle with a diameter of 1 mm and an outer circle with a diameter of 3 mm (Figure 1a). The parafoveal zone was divided into four sectors by the four radial lines: superior, temporal, inferior, and nasal. The following intraretinal layers were automatically generated, and their thickness measured using the macular cube scans: full thickness of the retina, ganglion cell complex, inner nuclear layer/outer plexiform layer (INL/OPL), outer nuclear layer/photoreceptor inner and outer segments (ONL/ISOS), and retinal pigment epithelium (RPE; Figure 1b).

Electroretinogram

The patients underwent an electroretinogram (ERG) using a flicker ERG testing device RETeval™ (LKC Technologies, Gaithersburg, MD, USA) without mydriasis. A sensor attached to the skin just below the eye was used to record the ERG. Waves of ERG were elicited by white light at a frequency of 28.3 Hz and an intensity of 8 troland-seconds, which was the default setting of the device. The contralateral eye was covered during the examination of the other eye. The values of amplitudes and implicit times were automatically displayed on the device.

Diagnosis and differentiation of DPN

Neuropathic symptoms and signs were assessed using Michigan neuropathy screening instrument (MNSI) scores²⁹ including physical examinations, e.g., ankle tendon reflexes (ATR), and measuring vibration sensations with a tuning fork. Subjects were screened for neurological dysfunction of the peripheral nervous system using the simple diagnostic criteria proposed by the Diabetic Neuropathy Study Group in Japan as described

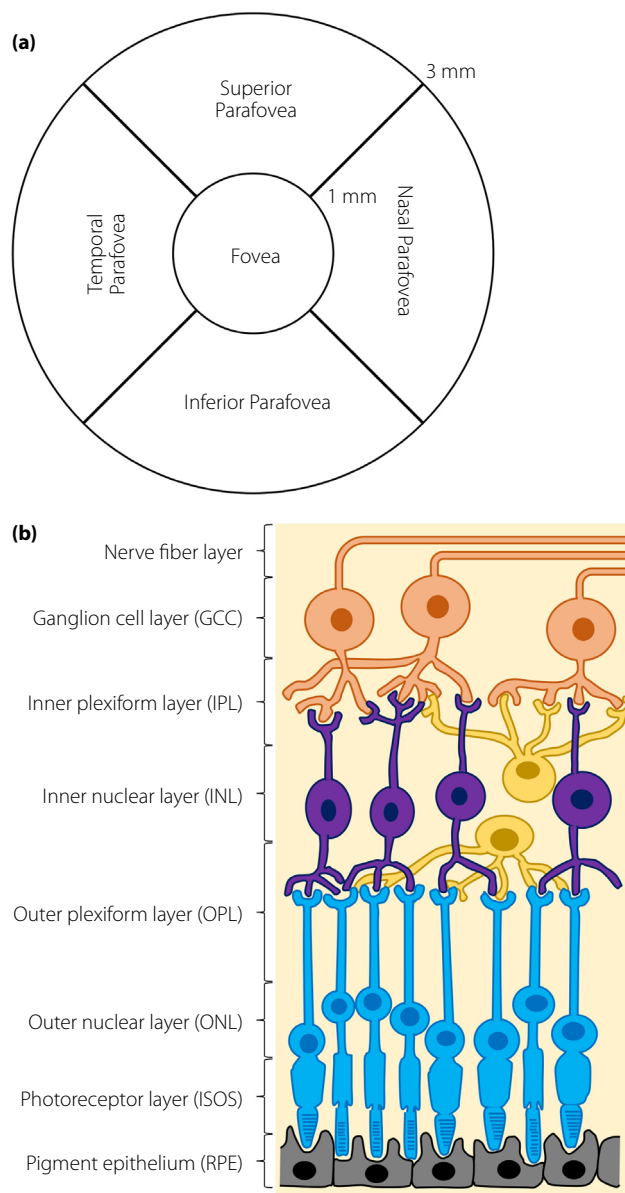


Figure 1 | The map of macular regions and schema of macular layers. (a) The map of macular regions. (b) The schema of macular layers.

previously³⁰. The criteria consist of a prerequisite condition and three neurological examination items. The prerequisite condition includes two items: (1) diagnosed as diabetes mellitus and (2) neuropathies other than diabetic polyneuropathy can be excluded. The criteria require any two or more of the following three items: (1) the presence of symptoms considered to be due to diabetic polyneuropathy, (2) decreased vibration in the bilateral medial malleoli, and (3) the decrease or disappearance of bilateral ankle tendon reflexes. Additionally, the criteria include important references in which, if either one of the following

reference items is met, even if the above criteria are not met, diabetic polyneuropathy can be diagnosed: (1) presence of any abnormality in two or more nerves in the nerve conduction study, (2) presence of clinically apparent diabetic autonomic dysfunction. However, in the protocol of the current study, these two reference items were not applied due to the lack of normal limits in each nerve conduction parameter and the lack of definitions of autonomic dysfunction.

The nerve conduction study was conducted utilizing a standard electromyography system (Neuropack X1, MEB-2312; Nihon Kohden, Tokyo, Japan). The NCS was carried out in an air-conditioned electrically shielded room and performed by trained technicians. The skin temperature was measured at the ankle, and the foot was warmed with a hot towel before testing when the temperature was below 32°C. The nerve conduction study was performed on the median, ulnar, tibial, and sural nerves. Clinical information for each subject was withheld from all examiners. During interpretation, NCS parameters were used to categorize diabetic polyneuropathy stages from 0 to 4 based on Baba's classification of the severity of diabetic polyneuropathy (BC)³¹. In brief, the subjects were divided into five stages; stage 0: normal without any NCS abnormalities; stage 1: mild neuropathy with the presence of any delay in tibial motor nerve conduction velocity (<40 m/s), sural SNCV (<40 m/s), tibial minimal F-wave latency ($>\{12.8 + 0.22 \times \text{Height (cm)}\}$ ms), or presence of A-wave; stage 2: moderate neuropathy with a decrease in sural SNAP amplitude <5 μ V; stage 3: between moderate to severe neuropathy with a decrease in sural SNAP amplitude <5 μ V and a decrease in tibial CMAP amplitude ≥ 2 to <5 mV; stage 4: severe neuropathy with a decrease in sural SNAP amplitude <5 μ V and a decrease in tibial CMAP amplitude <2 mV.

The coefficient of variation of RR intervals (CV_{R-R})

The CV_{R-R} was measured based on previously reported methods³². To analyze the CV_{R-R} , electrocardiogram recordings were collected in the supine position with normal or deep breathing for 1 min after 5 min of bed rest. The CV_{R-R} was calculated as follows:

$$CV_{R-R} (\%) = \frac{\text{(standard deviation of RR intervals)}}{\text{(mean RR intervals)}} \times 100.$$

Statistical analysis

SPSS Statistics version 20 for Windows (IBM SPSS, Chicago, IL, USA) was utilized for data analyses. Characteristics including age, sex, chemical laboratories, physiological findings, and NCS parameters were presented as raw data. Student's *t*-tests and chi-square tests with Yates' correction were used for analyses of differences in continuous and categorical variables, respectively. Correlations between optical coherence tomography parameters and other laboratory values were analyzed

using Pearson's correlation coefficients for normally distributed data and Spearman's correlation coefficients for non-normally distributed data. The diagnostic validity was analyzed using a receiver operating characteristic (ROC) curve and evaluated by the area under the ROC curve (AUROC).

RESULTS

Clinical characteristics of patients

The demographic and clinical characteristics of the study subjects are shown in Table 1. We enrolled 43 patients with a mean age of 61.5 ± 15.3 years. Based on Baba's classification, 6, 20, and 17 patients were classified as having no DPN, stage 1 mild DPN, and stage 2–4 moderate or more severe DPN, respectively. As the group with stage 0 DPN was too small for statistical analyses, hereafter we analyzed the differences between the group with stage 0 and 1 DPN and the group with stage 2–4 DPN. There was no significant difference in the age and body mass index (BMI) between patients with stage 2 or more severe DPN or with stage 0 and 1 DPN (age: stage 0 and 1 DPN 59.0 ± 16.3 years, stage 2 or more severe DPN 65.6 ± 12.2 , $P = 0.147$; BMI: stage 0 and 1 DPN: 25.5 ± 4.9 , stage 2 or more severe DPN 24.2 ± 5.1 , $P = 0.439$).

The changes in the thickness of retinal layers in patients with stage 2 or more severe DPN

The patients with stage 2 or more severe diabetic polyneuropathy showed deterioration of nerve conduction parameters in nerves of upper and lower extremities (Table 2). The thicknesses of some retinal layers decreased in patients with diabetes: foveal and parafoveal ONL/ISOS in patients with diabetes and parafoveal retinal pigment epithelium in patients with stage 2 or more severe diabetic polyneuropathy. The thicknesses of foveal and parafoveal INL/OPL increased in patients with diabetic polyneuropathy compared with patients with stage 0 and 1, but the thickness of parafoveal RPE decreased in patients with diabetic polyneuropathy (Figure 2).

Correlations between thicknesses of retinal layers and parameters of diabetes and its complications in the central zone with the fovea

In the central zone with the fovea, the full thickness of the retina positively correlated with height, systolic and diastolic blood pressures (SBP, DBP), and minimal F-wave latency in the tibial nerve; and negatively with sensory nerve conduction velocity (SNCV) in the sural nerve (Tables S1 and S2). Ganglion cell complex thickness positively correlated with HDL, u-ACR, and stage of diabetic retinopathy. The INL/OPL thickness positively correlated with stage of diabetic retinopathy and some nerve conduction parameters; and negatively with motor nerve conduction velocity (MNCV) and sensory nerve action potential (SNAP) in the median nerve. The ONL/ISOS thickness positively correlated with diastolic blood pressure, and negatively with maximal intima-media thickness in the common carotid artery. The thickness of the retinal pigment epithelium

Table 1 | Clinical characteristics of participants

Characteristics	Participants without diabetes	Patients with stage 0 or 1 DPN	Patients with stage 2 or more severe DPN
<i>N</i>	15	26	17
Age (years)	65.7 ± 7.5	59.0 ± 16.3	65.6 ± 12.2
Sex (men/women)	8/7	13/13	7/10
Duration of diabetes (years)	N/A	9.6 ± 10.2	12.6 ± 10.7
Height (cm)	161.6 ± 8.8	161.7 ± 7.6	161.7 ± 11.3
Body weight (kg)	59.9 ± 9.1	68.2 ± 15.5	63.9 ± 17.0
Body mass index (kg/m ²)	22.9 ± 2.9	26.0 ± 5.0	24.3 ± 5.7
Fasting blood glucose (mmol/L)	N/A	9.8 ± 4.5	11.1 ± 4.7
Casual blood glucose (mmol/L)	5.8 ± 0.6	N/A	N/A
Glycosylated hemoglobin (%)	N/A	9.8 ± 2.0	10.6 ± 2.4
Glycosylated hemoglobin (mmol/mol)	N/A	85.0 ± 24.5	81.1 ± 16.2
Glycoalbumin (%)	N/A	24.5 ± 6.1	26.1 ± 6.4
Serum C-peptide (nmol/L)	N/A	0.64 ± 0.52	1.11 ± 1.71
Urinary C-peptide (μmol/day)	N/A	19.6 ± 14.4	17.1 ± 17.4
Total cholesterol (mmol/L)	5.39 ± 0.88	4.84 ± 1.46	5.48 ± 2.25
High-density lipoprotein (mmol/L)	N/A	1.07 ± 0.40	1.22 ± 0.62
Low-density lipoprotein (mmol/L)	N/A	2.88 ± 1.05	2.55 ± 1.07
Triglyceride (mmol/L)	1.39 ± 0.69	2.20 ± 2.49	5.72 ± 12.77
Systolic blood pressure (mmHg)	136.7 ± 18.5	123.8 ± 14.8	146.6 ± 21.8*
Diastolic blood pressure (mmHg)	83.9 ± 13.1*	71.3 ± 11.5	78.4 ± 15.4
Urea nitrogen (mmol/L)	4.8 ± 0.8	5.1 ± 2.6	6.0 ± 3.0
Creatinine (μmol/L)	61.4 ± 14.7	64.4 ± 28.0	142.0 ± 266.9
Estimated glomerular filtration rate (mL/min/1.73 m ²)	82.3 ± 19.6	85.8 ± 30.0	80.1 ± 42.1
Diabetic retinopathy (NDR/SDR/PPDR/PDR)	N/A	26/0/0/0	6/4/1/6
Diabetic polyneuropathy (0/1/2/3/4) [†]	N/A	6/20/0/0/0	0/0/13/3/1
Diabetic nephropathy (1/2/3/4/5) [‡]	N/A	21/3/1/1/0	4/8/3/1/1

Categorical variables are given as number (percentage) while continuous variables are reported as mean ± standard deviation. N/A, not available; NDR, nondiabetic retinopathy; PDR, proliferative diabetic retinopathy; PPDR, preproliferative diabetic retinopathy; SDR, simple diabetic retinopathy. **P* < 0.05 compared with patients with stage 0 or 1 DPN. [†]Diagnosed and categorized based on Baba's classification on the severity of DPN. [‡]Diagnosed and categorized based on the classification of diabetic nephropathy 2014 established by the Joint Committee on Diabetic Nephropathy.

positively correlated with the amplitude of electroretinogram, SNAP in the median nerve, and compound muscle action potential (CMAP) in the ulnar and tibial nerve; and negatively with systolic blood pressure, HDL, stage of diabetic retinopathy, stage of diabetic polyneuropathy using BC, IMT, and baPWV.

Correlations between thicknesses of retinal layers and parameters of diabetes and its complications in the parafovea

In the parafoveal zone, a full thickness of the retina positively correlated with triglyceride and negatively with age and maximal IMT in the common carotid artery (Tables 3 and 4). The thickness of ganglion cell complex positively correlated with some nerve conduction velocity parameters; and negatively correlated with age, stage of diabetic retinopathy, stage of diabetic polyneuropathy, and baPWV. The thickness of INL/OPL positively correlated with the minimal F-wave latency in the tibial nerve, and negatively with CMAP in the ulnar nerve and SNCV in the sural nerve. The thickness of ONL/ISOS positively correlated with diastolic blood pressure, and CMAP in the

median nerve; and negatively with distal latency in the median nerve. The thickness of retinal pigment epithelium positively correlated with the amplitude of ERG, SNAP in the median nerve, and SNCV and SNAP in the sural nerve; and negatively with SBP, HDL, eGFR, stage of diabetic retinopathy, and stage of diabetic polyneuropathy or stage 2 ≤ of DPN using BC. The thickness of each layer appeared to show no evident difference among quadrants, but INL/OPL at the inferior parafovea might be sensitive to the changes of nerve conduction functions (Figure S1).

DISCUSSION

To elucidate the importance of neuroretinal impairment as a pathological aspect in diabetic polyneuropathy, we evaluated the correlation between the changes of thickness in layers of the retina and the nerve conduction study. As a result, we obtained three noteworthy results: first, the thickness of foveal and parafoveal INL/OPL increased but that of parafoveal retinal pigment epithelium decreased in patients with moderate to severe diabetic polyneuropathy compared with patients

Table 2 | Differences of retinal layer thicknesses between patients with stage 0 and 1 DPN and patients with stage 2 or more severe DPN

Measures	Participants without diabetes (n = 15)	Patients with stage 0 or 1 DPN (n = 26)	Patients with stage 2 or more severe DPN (n = 17)	P value between patients with or without stage 2 or more severe DPN
The thickness of retinal layers (µm)				
The full thickness of the retina, F	271 ± 38	265 ± 17	277 ± 29	0.152
The full thickness of the retina, P	336 ± 24	325 ± 14	327 ± 25	0.841
Ganglion cell complex, F	47 ± 16	46 ± 6	49 ± 8	0.206
Ganglion cell complex, P	111 ± 19	107 ± 9	104 ± 14	0.415
INL/OPL, F	48 ± 12	42 ± 7	48 ± 10	0.044
INL/OPL, P	72 ± 6	71 ± 5	75 ± 7	0.041
ONL/ISOS, F	133 ± 19 ^{**} , ^{***}	112 ± 17	111 ± 16	0.799
ONL/ISOS, P	99 ± 20 ^{**} , ^{***}	82 ± 11	83 ± 11	0.802
RPE, F	49 ± 2	48 ± 3	46 ± 5	0.142
RPE, P	52 ± 1 ^{***}	51 ± 2	49 ± 5	0.023
Flicker electroretinogram				
Implicit time (ms)	N/A	34 ± 2	36 ± 1	0.118
Amplitude (µV)	N/A	5.9 ± 2.8	5.4 ± 2.7	0.751
Nerve conduction study				
MNCV, median nerve (m/s)	N/A	54.7 ± 3.2	49.3 ± 3.4	<0.001
CMAP, median nerve (mV)	N/A	14.0 ± 4.2	12.3 ± 5.1	0.295
SNCV, median nerve (m/s)	N/A	48.3 ± 6.1	42.3 ± 5.4	0.004
SNAP, median nerve (µV)	N/A	38.6 ± 14.5	16.1 ± 11.6	<0.001
MNCV, ulnar nerve (m/s)	N/A	52.6 ± 3.9	46.6 ± 2.9	<0.001
CMAP, ulnar nerve (mV)	N/A	20.6 ± 11.8	11.3 ± 8.2	0.014
SNCV, ulnar nerve (m/s)	N/A	48.0 ± 5.2	44.4 ± 3.5	0.014
MNCV, tibial nerve (m/s)	N/A	43.3 ± 2.5	38.5 ± 3.0	<0.001
CMAP, tibial nerve (mV)	N/A	18.9 ± 4.3	10.5 ± 5.4	<0.001
Minimal F-wave latency, tibial nerve (ms)*	N/A	48.5 ± 5.3	51.3 ± 7.4	0.233
SNCV, sural nerve (m/s)	N/A	48.1 ± 4.5	39.6 ± 5.0	<0.001
SNAP, sural nerve (µV)	N/A	10.2 ± 5.0	1.5 ± 1.0	<0.001
Variability of R-R intervals				
CV _{R-R} , resting (%)	N/A	2.3 ± 1.2	2.2 ± 1.6	0.764
CV _{R-R} , deep breathing (%)	N/A	4.5 ± 3.0	3.0 ± 1.5	0.028
Parameters of diabetic nephropathy				
eGFR (mL/min/1.73 m ²)	N/A	89.0 ± 30.4	80.1 ± 42.1	0.495
u-ACR (mg/g)	N/A	34.2 ± 80.8	577.4 ± 1686.1	0.120
Ln(u-ACR)	N/A	2.6 ± 1.1	3.9 ± 2.0	0.020
Parameters of atherosclerosis				
Mean IMT (mm)	N/A	1.08 ± 0.47	1.49 ± 0.64	0.047
Maximal IMT (mm)	N/A	1.73 ± 0.77	2.31 ± 1.01	0.077
Brachial-ankle pulse wave velocity (m/s)	N/A	1659 ± 499	1733 ± 379	0.609
Ankle-brachial index	N/A	1.07 ± 0.17	1.11 ± 0.17	0.516
Toe-brachial index	N/A	0.68 ± 0.16	0.64 ± 0.14	0.438

Variables are reported as mean ± standard deviation. CMAP, compound muscle action potential; CV_{R-R}, coefficient of variation of R-R intervals; DPN, diabetic polyneuropathy; eGFR, estimated glomerular filtration rate; F, central zone with the fovea; IMT, intima-media thickness; INL/OPL, inner nuclear layer/outer plexiform layer; Ln, natural logarithm; MNCV, motor nerve conduction velocity; N/A, not available; ONL/ISOS, outer nuclear layer/photoreceptor inner and outer segments; P, parafovea; RPE, retinal pigment epithelium; SNAP, sensory nerve action potential; SNCV, sensory nerve conduction velocity; u-ACR, urine albumin-to-creatinine ratio. *Minimal F-wave latencies were corrected with height using the following formula: height (cm)/160 × latency (s). Significant P values are shown in bold. **P < 0.05 versus patients with stage 0 or 1 DPN. ***P < 0.05 versus patients with stage 2 or more severe DPN.

without or subclinical (stage 1) DPN; second, a decrease in the thickness of parafoveal ganglion cell complex and foveal and parafoveal retinal pigment epithelium positively correlated with deterioration of nerve functions in the nerve conduction

study; third, a decrease in the thicknesses of parafoveal ganglion cell complex and foveal RPE positively correlated with an increase in the parameters of atherosclerosis and cardiovascular risk factors.

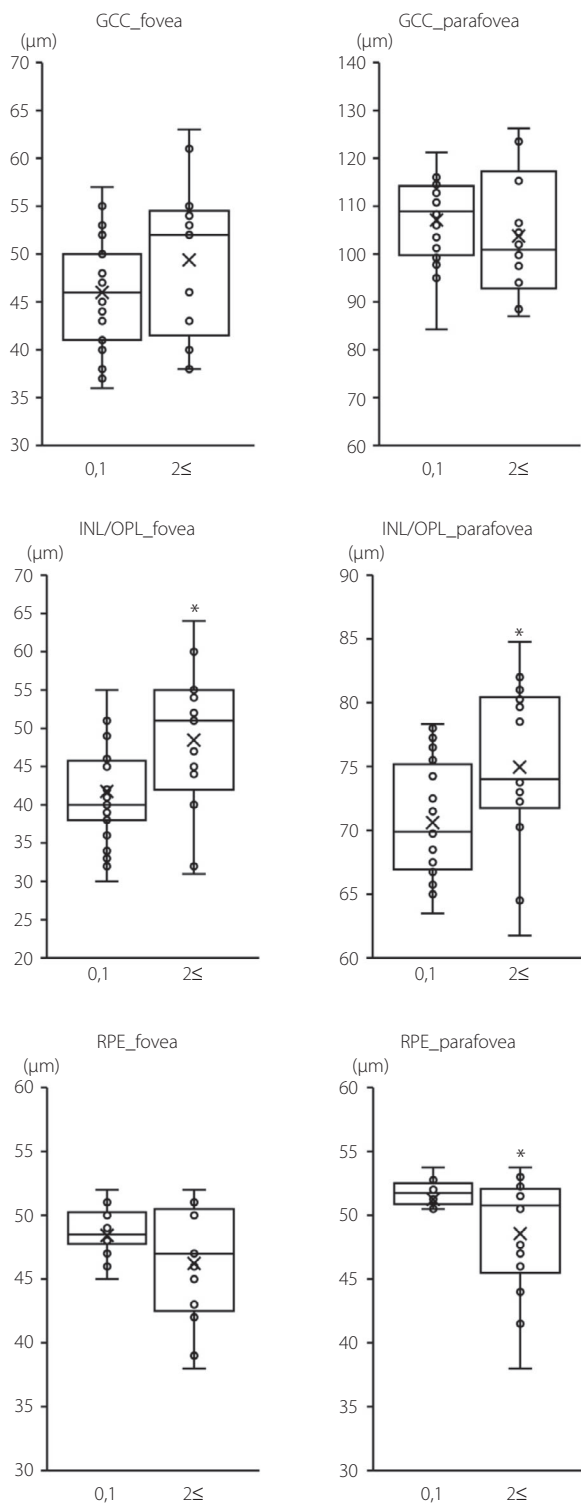


Figure 2 | The changes in thickness of retinal layers in patients with stage 2 or more severe DPN. 0, 1: stage 0 and 1 diabetic polyneuropathy (DPN) according to Baba's classification (BC). 2≤: stage 2 or more severe DPN according to BC. GCC, ganglion cell complex; INL/OPL, inner nuclear layer/outer plexiform layer; RPE, retinal pigment epithelium. * $P < 0.05$ compared with stage 0 and 1 DPN.

Although most previous papers have reported a decrease in retinal thickness, especially the thickness in ganglion cell complex, in patients with diabetes, we found an increase of INL/OPL in patients with diabetic polyneuropathy. Additionally, in the previous study in which the relationship between the progression of diabetic retinopathy and retinal layers was investigated³³, Joltikov *et al.* reported an increase of INL/OPL in patients with moderate diabetic retinopathy. Although there is a difference in that the current paper focused on neuropathy and the previous paper focused on retinopathy, it can be said that the reliability of the results is justifiable because similar results were obtained in similar subjects. As the inner nuclear layer consists of the cell bodies of horizontal cells, bipolar cells, amacrine cells, interplexiform neurons, and Müller cells, we surmised that Müller cells, the principal glial cell in the retina, caused the increase of thickness in INL/OPL. In a previous clinical paper, electron microscopic findings verified a reactive gliosis, which is a progressive transformation from the Müller cell phenotype to a poorly differentiated glial cell phenotype, and the proliferation of glial cell processes in patients with diabetes³⁴. Additionally, an animal experiment using an organotypic culture of mouse retina clarified that Müller cells in the inner nuclear layer initiated their proliferation when induced by retinal injury³⁵. Although the details of molecular mechanisms involved in the Müller cell response to hyperglycemia have not been thoroughly investigated, a previous paper indicated the association of the advanced glycation end-products in Müller cells³⁶. Considering these reports, the increase in the thickness of INL/OPL might be generated by the reactive gliosis of Müller cells in the inner nuclear layer. Further research is essential to understand the precise mechanism of the increase in INL/OPL.

Our second finding, the decrease in the thicknesses of parafoveal ganglion cell complex and foveal and parafoveal RPE in patients with nerve conduction dysfunction, was consistent with previous reports regarding the ganglion cell complex^{6,8,37}. Thus, the loss of ganglion cells, the third-order neurons in the neuroretina, could be evidence of neurodegeneration in patients with diabetes. However, the change of retinal pigment epithelium in patients with diabetes is less known. A recent paper found an increase of thickness in RPE in patients with diabetes compared with healthy subjects³⁸, but other papers reported no significant change of RPE in subjects with or without diabetes³⁹, or a decrease of RPE thickness in patients with diabetic retinopathy compared with normal individuals⁴⁰. This discrepancy might be introduced by differences of study participants, insufficient scales of these studies, or differences of a built-in automatic segmentation software used in each study; in fact, the mean thickness of RPE distributed less than 20 µm to more than 80 µm in these studies. As RPE is the epithelial layer between photoreceptors and vasculature in the choroid, forms a blood-retinal barrier, and supports photoreceptor function by providing growth factors⁴¹ and daily phagocytosis⁴², dysfunction of RPE would promote retinal degeneration. In animal

Table 3 | Correlations between retinal layer thicknesses and parameters of diabetic polyneuropathy in the parafoveal zone

Characteristics and measures	Full thickness of the retina	GCC	INL/OPL	ONL/ISOS	RPE
Physical signs and symptoms of DPN					
Presence of neuropathic symptoms ¹	-0.114	-0.216	0.086	0.063	-0.364*
Abnormal appearance of feet	-0.003	-0.221	0.288	-0.197	-0.381*
Ulceration of feet	0.200	0.238	0.238	-0.097	-0.121
Decrease or disappearance of bilateral ATRs	-0.068	-0.241	0.017	0.099	-0.036
Decreased vibration ²	-0.082	-0.134	0.144	-0.050	-0.145
MNSI questionnaire score	-0.006	-0.067	0.251	0.112	0.024
MNSI physical assessment score	-0.091	-0.208	0.142	0.005	-0.140
2 ≤ MNSI physical assessment score	-0.020	-0.170	0.098	-0.040	-0.066
Existence of DPN diagnosed using SDCJ	-0.060	-0.167	0.028	0.101	-0.247
Nerve conduction study					
MNCV, median nerve	-0.019	0.089	-0.224	0.167	-0.003
CMAP, median nerve	0.171	0.102	-0.165	0.369*	0.123
Distal latency, median nerve	0.001	0.148	0.235	-0.338*	0.025
SNCV, median nerve	-0.068	0.015	-0.257	0.190	0.128
SNAP, median nerve	0.131	0.286	-0.257	0.121	0.330*
MNCV, ulnar nerve	0.049	0.305*	-0.203	0.005	0.103
CMAP, ulnar nerve	-0.132	0.170	-0.313*	-0.215	0.259
Distal latency, ulnar nerve	0.139	-0.091	0.145	-0.050	-0.082
SNCV, ulnar nerve	0.083	0.205	-0.075	0.148	0.046
MNCV, tibial nerve	0.210	0.317*	-0.140	0.163	0.147
CMAP, tibial nerve	0.281	0.493*	-0.088	0.045	0.270
Minimal F-wave latency, tibial nerve ³	0.273	0.102	0.337*	0.074	-0.063
A-wave, tibial nerve	0.049	0.090	0.133	-0.227	0.059
SNCV, sural nerve	-0.086	0.005	-0.330*	-0.019	0.407**
SNAP, sural nerve	-0.026	0.079	-0.283	-0.021	0.345*
Stages of DPN using BC	-0.179	-0.351*	0.196	-0.016	-0.418**
Stage 2 ≤ of DPN in BC	-0.105	-0.263	0.207	0.015	-0.367*
Corneal confocal microscopy					
Corneal nerve fiber density	0.349	0.403	0.026	0.060	0.063
Corneal nerve branch density	-0.058	-0.123	-0.431	0.309	-0.253
Corneal nerve fiber length	0.333	0.331	-0.154	0.283	-0.052
Corneal total branch density	0.059	0.041	-0.312	0.306	-0.177
Corneal nerve fiber area	0.120	0.073	-0.076	0.243	-0.107
Corneal nerve fiber width	-0.105	-0.184	-0.163	0.281	0.024
Corneal nerve fractal dimension	0.241	0.161	-0.199	0.290	-0.084
Variability of R-R intervals					
CV _{R-R} resting	-0.220	-0.142	-0.096	-0.158	0.014
CV _{R-R} deep breathing	-0.042	0.039	0.086	-0.208	0.023

Variables are reported as coefficients of correlation. 1: Bilateral numbness, pain, paresthesia, or decreased sensation in the tips of toes and bottom of feet; 2: Decreased vibration in the bilateral medial malleoli; 3: Minimal F-wave latencies were corrected with height using the following formula; height (cm)/160 × latency (s). Significant correlation values are shown in bold. ATRs, ankle tendon reflexes; BC, Baba's classification on the severity of DPN; CMAP, compound muscle action potential; CV_{R-R}, coefficient of variation of R-R intervals; DPN, diabetic polyneuropathy; GCC, ganglion cell complex; INL/OPL, inner nuclear layer/outer plexiform layer; MNCV, motor nerve conduction velocity; MNSI, Michigan neuropathy screening instrument; ONL/ISOS, outer nuclear layer/photoreceptor inner and outer segments; RPE, retinal pigment epithelium; SDCJ, the simple diagnostic criteria proposed by Diabetic Neuropathy Study Group in Japan; SNAP, sensory nerve action potential; SNCV, sensory nerve conduction velocity. *P < 0.05. **P < 0.01.

models of diabetes, a loss of structural integrity in RPE was also verified⁴³. We should perform further research focusing on the changes in RPE in the future.

The third finding indicated that atherosclerosis and its risk factors promoted the degeneration of the ganglion cell complex

and RPE in diabetic patients. Little is known about the relationship between atherosclerosis or cardiovascular risk factors and retinal thickness. Although it was reported that the thickness of the retinal nerve fiber layer around the optic disc decreased in patients with hypertension or increased IMT^{44,45}, no report has

Table 4 | Correlations between retinal layer thicknesses and parameters of diabetes and its complications except for diabetic polyneuropathy in the parafoveal zone

Characteristics and measures	Full thickness of the retina	GCC	INL/OPL	ONL/ISOS	RPE
Physical and social backgrounds					
Age	-0.434**	-0.344*	-0.170	-0.115	0.086
Sex	-0.231	0.008	-0.124	-0.182	-0.254
Height	0.277	0.166	0.284	0.090	0.054
Body weight	0.148	0.100	-0.022	0.087	0.334*
Body mass index	0.017	0.017	-0.189	0.047	0.372*
History of smoking	0.172	0.245	0.164	0.054	0.063
History of cardiovascular diseases	-0.030	0.097	0.087	0.019	-0.073
History of peripheral artery disease	0.199	0.236	0.236	-0.099	-0.123
Metabolic parameters associated with cardiovascular risks					
Systolic blood pressure	-0.020	-0.176	0.240	0.119	-0.342*
Diastolic blood pressure	0.212	-0.063	0.072	0.310*	-0.103
Total cholesterol	0.204	-0.015	0.178	0.137	-0.213
Triglyceride (log)	0.354*	0.252	0.168	0.264	0.005
High-density lipoprotein	0.053	-0.186	0.171	0.065	-0.588**
Low-density lipoprotein	0.159	-0.021	0.090	0.123	-0.093
Duration of diabetes	-0.008	-0.137	0.042	0.104	-0.060
Glycosylated hemoglobin	0.164	0.039	0.094	0.023	0.011
Glycoalbumin	0.067	-0.041	0.177	-0.192	0.029
Fasting blood glucose	0.179	0.134	0.278	-0.064	-0.232
Serum C-peptide	-0.300	-0.276	0.139	-0.166	-0.115
Urinary C-peptide, /day	-0.035	-0.047	-0.025	-0.018	0.137
Parameters of diabetic nephropathy (DN)					
Urea nitrogen	-0.133	-0.249	0.124	0.013	0.075
Creatinine	-0.252	-0.264	0.172	-0.138	-0.074
eGFR	0.139	0.237	0.016	-0.003	-0.392*
Stages of DN	-0.022	-0.380*	0.254	0.140	-0.140
Existence of DN	0.004	-0.359*	0.202	0.166	-0.163
Ln(u-ACR)	0.061	-0.276	0.237	0.034	-0.269
Urinary L-FABP/creatinine	-0.167	-0.190	0.203	-0.104	-0.088
Parameters of diabetic retinopathy (DR)					
Stages of DR	0.140	-0.070	0.284	0.146	-0.417*
Implicit time of electroretinogram	-0.465	-0.385	-0.033	-0.259	0.174
Amplitude of electroretinogram	0.553	0.558	0.134	0.056	0.640*
Carotid ultrasonography					
Maximal IMT, common carotid artery	-0.352*	-0.210	0.096	-0.251	-0.229
Maximal IMT, carotid bifurcation	-0.184	-0.097	0.105	-0.205	-0.046
Maximal IMT, internal carotid artery	-0.099	0.039	0.104	-0.049	-0.198
Mean IMT	-0.261	-0.115	0.123	-0.217	-0.169
Maximal IMT	-0.298	-0.269	0.069	-0.066	-0.229
Existence of plaque	-0.298	-0.359*	-0.116	-0.099	-0.163
Pulse wave analysis					
baPWV	-0.301	-0.374*	-0.071	-0.062	-0.209
ABI	0.087	0.038	0.143	0.123	-0.069
TBI	0.025	-0.052	-0.214	0.187	0.064

Variables are reported as coefficients of correlation. Significant correlation values are shown in bold. ABI, Ankle-brachial index; eGFR, estimated glomerular filtration rate; GCC, ganglion cell complex; IMT, intima-media thickness. baPWV, Brachial-ankle pulse wave velocity; INL/OPL, inner nuclear layer/outer plexiform layer; L-FABP, liver fatty acid-binding protein; Ln, natural logarithm; ONL/ISOS, outer nuclear layer/photoreceptor inner and outer segments; RPE, retinal pigment epithelium; TBI, Toe-brachial index; u-ACR, urinary albumin-to-creatinine ratio. * $P < 0.05$. ** $P < 0.01$.

analyzed the neuroretinal layers around the macula with detailed segmentation. Regarding the change in RPE, the anti-atherosclerotic drug statin was reported to be effective in

improving the RPE and choroid function in high-fat-fed atherogenic rodents⁴⁶ and in age-related macular degeneration which has similarities in risk factors and pathogenesis with

atherosclerosis⁴⁷. However, there is no report that directly suggests a change in the thickness of RPE. Therefore, the current study will be the first report indicating the relationship between cardiovascular risk factors and changes in ganglion cell complex and retinal pigment epithelium.

In the present study, we hypothesized that the neuroretina may share a similar pathology to diabetic polyneuropathy. As the hypothesis appears to be supported by the current results, in which the decrease in the thickness of ganglion cell complex and RPE correlated with the decrease of nerve conduction parameters. However, as this study is cross-sectional, it is hard to speculate a causal relationship between retina and neuropathy. Therefore, we should consider conducting prospective studies with a larger number of patients with diabetes and participants without diabetes. Additionally, the novel finding of an increase in the thickness of INL/OPL in diabetic polyneuropathy patients should be verified with large-scale and prospective trials.

In conclusion, depending on the progress of diabetic polyneuropathy, the layers of the retina exhibited different directional changes; the ganglion cell complex and RPE became thinner and the INL/OPL became thicker. Although the mechanism of the alterations is little known, the fact that the retina changes with the progression of diabetic polyneuropathy will increase the possibility of elucidating the pathology of diabetic polyneuropathy and diabetic retinopathy. As the neuroretina around the macula allows detailed observation of neuronal and glial behaviors in the peripheral sensory tissue, close attention to these retinal changes is possible, and might provide important signs for the diagnosis and pathological investigations of diabetic polyneuropathy.

ACKNOWLEDGMENTS

The authors thank nurses and staff from the Division of Diabetes, the Department of Internal Medicine, and the Department of Ophthalmology at Aichi Medical University Hospital. The authors are particularly grateful to Carson Maynard (Department of Philosophy, University of Michigan, Ann Arbor, MI, USA) for his editorial assistance. T.H. acknowledges the following grants and foundations for their support to his research management: a Grant-in-Aid for Scientific Research (15H06720) from the Ministry of Education, Culture, Sports, Science and Technology (MEXT), Grants for young researchers from Japan Association for Diabetes Education and Care, the Manpei Suzuki Diabetes Foundation, Japan Diabetes Foundation, Suzuken Memorial Foundation, the Nitto Foundation, and Aichi Medical University Aikeikai.

DISCLOSURE

The authors declare no conflict of interest.

FUNDING

This research did not receive any specific grant from funding agencies in the public, commercial, or not-for-profit sectors.

REFERENCES

- American Diabetes Association. 11. Microvascular complications and foot care: standards of medical care in diabetes-2020. *Diabetes Care* 2020; 43(Suppl 1): S135–S151.
- Iadecola C. The neurovascular unit coming of age: a journey through neurovascular coupling in health and disease. *Neuron* 2017; 96: 17–42.
- Antonetti DA, Klein R, Gardner TW. Diabetic retinopathy. *N Engl J Med* 2012; 366: 1227–1239.
- van Dijk HW, Kok PH, Garvin M, et al. Selective loss of inner retinal layer thickness in type 1 diabetic patients with minimal diabetic retinopathy. *Invest Ophthalmol Vis Sci* 2009; 50: 3404–3409.
- Barber AJ, Lieth E, Khin SA, et al. Neural apoptosis in the retina during experimental and human diabetes. Early onset and effect of insulin. *J Clin Invest* 1998; 102: 783–791.
- El-Fayoumi D, Badr Eldine NM, Esmael AF, et al. Retinal nerve fiber layer and ganglion cell complex thicknesses are reduced in children with type 1 diabetes with no evidence of vascular retinopathy. *Invest Ophthalmol Vis Sci* 2016; 57: 5355–5360.
- Jonsson KB, Frydkjaer-Olsen U, Grauslund J. Vascular changes and neurodegeneration in the early stages of diabetic retinopathy: which comes first? *Ophthalmic Res* 2016; 56: 1–9.
- Thangamathesvaran L, Kommana SS, Duong K, et al. Ganglion cell complex loss in patients with type 1 diabetes: a 36-month retrospective study. *Oman J Ophthalmol* 2019; 12: 31–36.
- Lim HB, Shin YI, Lee MW, et al. Ganglion cell – inner plexiform layer damage in diabetic patients: 3-year prospective, longitudinal, observational study. *Sci Rep* 2020; 10: 1470.
- Lavia C, Couturier A, Erginay A, et al. Reduced vessel density in the superficial and deep plexuses in diabetic retinopathy is associated with structural changes in corresponding retinal layers. *PLoS One* 2019; 14: e0219164.
- Lynch SK, Abramoff MD. Diabetic retinopathy is a neurodegenerative disorder. *Vision Res* 2017; 139: 101–107.
- Oshitari T, Yamamoto S, Hata N, et al. Mitochondria- and caspase-dependent cell death pathway involved in neuronal degeneration in diabetic retinopathy. *Br J Ophthalmol* 2008; 92: 552–556.
- Lieth E, Barber A, Xu B, et al. Glial reactivity and impaired glutamate metabolism in short-term experimental diabetic retinopathy. Penn State Retina Research Group. *Diabetes* 1998; 47: 815–820.
- Doustar J, Torbati T, Black KL, et al. Optical coherence tomography in Alzheimer's disease and other neurodegenerative diseases. *Front Neurol* 2017; 8: 701.
- Chan VTT, Sun Z, Tang S, et al. Spectral-domain OCT measurements in Alzheimer's disease: a systematic review and meta-analysis. *Ophthalmology* 2019; 126: 497–510.

16. Moreno-Ramos T, Benito-Leon J, Villarejo A, *et al.* Retinal nerve fiber layer thinning in dementia associated with Parkinson's disease, dementia with Lewy bodies, and Alzheimer's disease. *J Alzheimers Dis* 2013; 34: 659–664.
17. Almeida ALM, Pires LA, Figueiredo EA, *et al.* Correlation between cognitive impairment and retinal neural loss assessed by swept-source optical coherence tomography in patients with mild cognitive impairment. *Alzheimers Dement (Amst)* 2019; 11: 659–669.
18. Chen Q, Tan F, Wu Y, *et al.* Characteristics of retinal structural and microvascular alterations in early type 2 diabetic patients. *Invest Ophthalmol Vis Sci* 2018; 59: 2110–2118.
19. Tekin K, Inanc M, Kurnaz E, *et al.* Quantitative evaluation of early retinal changes in children with type 1 diabetes mellitus without retinopathy. *Clin Exp Optom* 2018; 101: 680–685.
20. Srinivasan S, Dehghani C, Pritchard N, *et al.* Corneal and retinal neuronal degeneration in early stages of diabetic retinopathy. *Invest Ophthalmol Vis Sci* 2017; 58: 6365–6373.
21. Young MJ, Boulton AJ, MacLeod AF, *et al.* A multicentre study of the prevalence of diabetic peripheral neuropathy in the United Kingdom hospital clinic population. *Diabetologia* 1993; 36: 150–154.
22. Shahidi AM, Sampson GP, Pritchard N, *et al.* Retinal nerve fibre layer thinning associated with diabetic peripheral neuropathy. *Diabet Med* 2012; 29: e106–e111.
23. Srinivasan S, Pritchard N, Sampson GP, *et al.* Diagnostic capability of retinal thickness measures in diabetic peripheral neuropathy. *J Optom* 2017; 10: 215–225.
24. Hafner J, Zadrazil M, Grisold A, *et al.* Retinal and corneal neurodegeneration and their association with systemic signs of peripheral neuropathy in type 2 diabetes. *Am J Ophthalmol* 2020; 209: 197–205.
25. Ishikawa H, Stein DM, Wollstein G, *et al.* Macular segmentation with optical coherence tomography. *Invest Ophthalmol Vis Sci* 2005; 46: 2012–2017.
26. Haneda M, Utsunomiya K, Koya D, *et al.* A new classification of diabetic nephropathy 2014: a report from joint committee on diabetic nephropathy. *J Diabetes Investig* 2015; 6: 242–246.
27. Imai E, Horio M, Nitta K, *et al.* Estimation of glomerular filtration rate by the MDRD study equation modified for Japanese patients with chronic kidney disease. *Clin Exp Nephrol* 2007; 11: 41–50.
28. Early Treatment Diabetic Retinopathy Study Research Group. Grading diabetic retinopathy from stereoscopic color fundus photographs – an extension of the modified Airlie House classification. ETDRS report number 10. *Ophthalmology* 1991; 98(5 Suppl): 786–806.
29. Feldman EL, Stevens MJ, Thomas PK, *et al.* A practical two-step quantitative clinical and electrophysiological assessment for the diagnosis and staging of diabetic neuropathy. *Diabetes Care* 1994; 17: 1281–1289.
30. Yasuda H, Sanada M, Kitada K, *et al.* Rationale and usefulness of newly devised abbreviated diagnostic criteria and staging for diabetic polyneuropathy. *Diabetes Res Clin Pract* 2007; 77(Suppl 1): S178–S183.
31. Himeno T, Kamiya H, Nakamura J. Lumos for the long trail: strategies for clinical diagnosis and severity staging for diabetic polyneuropathy and future directions. *J Diabetes Investig* 2020; 11(1): 5–16.
32. Kageyama S, Taniguchi I, Tanaka S, *et al.* A critical level of diabetic autonomic neuropathy. *Tohoku J Exp Med* 1983; 141(Suppl): 479–483.
33. Joltikov K, de Castro V, Davila J, *et al.* Multidimensional functional and structural evaluation reveals neuroretinal impairment in early diabetic retinopathy. *Invest Ophthalmol Vis Sci* 2017; 58(6): BIO277–BIO290.
34. Feher J, Taurone S, Spoletini M, *et al.* Ultrastructure of neurovascular changes in human diabetic retinopathy. *Int J Immunopathol Pharmacol* 2018; 31: 394632017748841.
35. Sardar Pasha SPB, Munch R, Schafer P, *et al.* Retinal cell death dependent reactive proliferative gliosis in the mouse retina. *Sci Rep* 2017; 7: 9517.
36. Zong H, Ward M, Madden A, *et al.* Hyperglycaemia-induced pro-inflammatory responses by retinal Müller glia are regulated by the receptor for advanced glycation end-products (RAGE). *Diabetologia* 2010; 53: 2656–2666.
37. Wanek J, Blair NP, Chau FY, *et al.* Alterations in retinal layer thickness and reflectance at different stages of diabetic retinopathy by en face optical coherence tomography. *Invest Ophthalmol Vis Sci* 2016; 57: OCT341–OCT3417.
38. Xia Z, Chen H, Zheng S. Alterations of retinal pigment epithelium-photoreceptor complex in patients with type 2 diabetes mellitus without diabetic retinopathy: a cross-sectional study. *J Diabetes Res* 2020; 2020: 9232157.
39. Tavares Ferreira J, Alves M, Dias-Santos A, *et al.* Retinal neurodegeneration in diabetic patients without diabetic retinopathy. *Invest Ophthalmol Vis Sci* 2016; 57: 6455–6460.
40. Wang XN, Li ST, Li W, *et al.* The thickness and volume of the choroid, outer retinal layers and retinal pigment epithelium layer changes in patients with diabetic retinopathy. *Int J Ophthalmol* 2018; 11: 1957–1962.
41. Whitmire W, Al-Gayyar M, Abdelsaid M, *et al.* Alteration of growth factors and neuronal death in diabetic retinopathy: what we have learned so far. *Mol Vis* 2011; 17: 300–308.
42. Lakkaraju A, Umapathy A, Tan L, *et al.* The cell biology of the retinal pigment epithelium. *Prog Retin Eye Res* 2020; 78: 100846.
43. Aizu Y, Oyanagi K, Hu J, *et al.* Degeneration of retinal neuronal processes and pigment epithelium in the early stage of the streptozotocin-diabetic rats. *Neuropathology* 2002; 22: 161–170.
44. Sahin SB, Sahin OZ, Ayaz T, *et al.* The relationship between retinal nerve fiber layer thickness and carotid intima media thickness in patients with type 2 diabetes mellitus. *Diabetes Res Clin Pract* 2014; 106: 583–589.

45. Sahin OZ, Sahin SB, Ayaz T, *et al.* The impact of hypertension on retinal nerve fiber layer thickness and its association with carotid intima media thickness. *Blood Press* 2015; 24: 178–184.
46. Barathi VA, Yeo SW, Guymer RH, *et al.* Effects of simvastatin on retinal structure and function of a high-fat atherogenic mouse model of thickened Bruch's membrane. *Invest Ophthalmol Vis Sci* 2014; 55: 460–468.
47. Vavvas DG, Daniels AB, Kapsala ZG, *et al.* Regression of some high-risk features of age-related macular degeneration (AMD) in patients receiving intensive statin treatment. *EBioMedicine* 2016; 5: 198–203.

SUPPORTING INFORMATION

Additional supporting information may be found online in the Supporting Information section at the end of the article.

Table S1 | Correlations between retinal layer thicknesses and parameters of diabetic polyneuropathy in the central zone with the fovea.

Table S2 | Correlations between retinal layer thicknesses and parameters of diabetes and its complications except for diabetic polyneuropathy in the central zone with the fovea.

Figure S1 | A heat map representing coefficients of correlation between parameters of diabetes and its complications and the parafoveal thicknesses of retinal layers.